energies

Article

A Novel Denoising Auto-Encoder-Based Approach for Non-Intrusive Residential Load Monitoring

Xi He [1,*], Heng Dong [1], Wanli Yang [2] and Jun Hong [1]

[1] Department of Electrical and Information Engineering, Hunan Institute of Technology, Hengyang 421002, China; 2014001882@hnit.edu.cn (H.D.); 2013001763@hnit.edu.cn (J.H.)
[2] Department of Electrical and Information Engineering, Hunan University, Changsha 410006, China; yangwanli542@hnu.edu.cn
* Correspondence: 2019001008@hnit.edu.cn

Abstract: Mounting concerns pertaining to energy efficiency have led to the research of load monitoring. By Non-Intrusive Load Monitoring (NILM), detailed information regarding the electric energy consumed by each appliance per day or per hour can be formed. The accuracy of the previous residential load monitoring approach relies heavily on the data acquisition frequency of the energy meters. It brings high overall cost issues, and furthermore, the differentiating algorithm becomes much more complicated. Based on this, we proposed a novel non-Intrusive residential load disaggregation method that only depends on the regular data acquisition speed of active power measurements. Additionally, this approach brings some novelties to the traditionally used denoising Auto-Encoder (dAE), i.e., the reconfiguration of the overlapping parts of the sliding windows. The median filter is used for the data processing of the overlapping window. Two datasets, i.e., the Reference Energy Disaggregation Dataset (REDD) and TraceBase, are used for test and validation. By numerical testing of the real residential data, it proves that the proposed method is superior to the traditional Factorial Hidden Markov Model (FHMM)-based approach. Furthermore, the proposed method can be used for energy data, disaggregation disregarding the brand and model of each appliance.

Keywords: load disaggregation; denoising auto-encoder; REDD dataset; TraceBase dataset; machine learning

Citation: He, X.; Dong, H.; Yang, W.; Hong, J. A Novel Denoising Auto-Encoder-Based Approach for Non-Intrusive Residential Load Monitoring. *Energies* **2022**, *15*, 2290. https://doi.org/10.3390/en15062290

Academic Editor: Djaffar Ould-Abdeslam

Received: 14 February 2022
Accepted: 18 March 2022
Published: 21 March 2022

1. Introduction

At present, the household electric meter can only measure total electricity consumption, and not the individual electric consumption of various loads. Energy disaggregation is the computational process of distinguishing individual power consumptions of an electrical appliance from the mixed measurement. The application of NILM can help households reduce their cost of energy consumption. According to related studies, with the energy consumption information of each appliance, users can realize energy conservation of more than 12% [1]. In addition, with the increasing installation of renewable energy, the distribution network needs faster and more accurate demand-side response capability. The realization of this capability depends on load disaggregation [2,3].

The load disaggregation of residential electrical equipment is an important direction of smart grid research. The user's electrical equipment has the characteristics of wide variety, large scale, and large differences in the load characteristics [4]. At present, with the pilot and promotion of load disaggregation for residential users, many local load monitoring devices have been deployed. In actual use, it is found that load monitoring devices generally undergo sample data training or learning process in advance. The difficulties in field use are threefold: firstly, due to the low efficiency of the algorithm, the real-time performance of load disaggregation is difficult to guarantee; secondly, due to the wide variety of electrical equipment and complex working conditions, it is difficult to find an algorithm to accurately identify each electrical equipment, and thirdly, when users deploy new devices, they often cannot be identified correctly, which brings great limitations to field usage. Therefore, it is necessary to consider adopting a method to solve the problem of online disaggregation and synchronization of local load disaggregation equipment [5,6].

Load disaggregation can be divided into intrusive methods based on hardware devices and non-intrusive methods based on software algorithms (Nonintrusive Load Monitoring—NILM) [7–9]. In 1992, Hart addressed the energy data disaggregation problem for the first time using Finite State Machine (FSM), which led to the new approaches based on Hidden Markov Models (HMM), and Factorial Hidden Markov Models (FHMM) [10–13]. The essence of these methods is to model the specific electrical signatures or features of each device, either manually or automatically. Ref. [14] proposed an intrusive load disaggregation method based on distributed power Measurement and Actuation Units (MAUs). MAUs are connected between the device plug and the power outlet. The MAU device can measure the power consumption of a single device and control the power failure of the device for demand-side response. Because the invasive method requires additional installation of equipment, the user's responsiveness is relatively low. More research on load disaggregation focus on non-invasive methods. For example, [15] separates the high frequency collected load current data to build a load feature library to realize non-intrusive automatic load monitoring of adaptive users and [16] proposes a non-intrusive load disaggregation method based on generalized regression neural network. This method needs to obtain data such as power, harmonics, switching time, and so on. Ref. [17] proposes separating the superimposed loads based on the transient reactive power characteristics of the load at opening moment, and the coded Particle Swarm Algorithm (E-PSO) is deployed for disaggregation. The above studies all have high load disaggregation accuracy; however, all of them have high requirements for data measurement. Whether it is the high-frequency load current data or the transient waveform when the load is turned on, the ordinary electric meter needs to be transformed before these data can be obtained, adding additional cost to the customers.

In recent years, some scholars proposed to only use low-frequency single measurement for load disaggregation [18–21]. Ref. [18] uses the effective value of current to identify the load, and Ref. [19] only uses the steady-state time domain active and reactive power to identify the turn-on or turn-off status of electrical equipment. A common defect of these methods is that the disaggregation accuracy is poor when multiple loads with similar steady-state waveforms are turned on at the same time.

In terms of disaggregation algorithms, load disaggregation based on machine learning methods is known as a research hotspot [22–28]. Various mature machine learning algorithms are applied to load disaggregation, such as Factorial Hidden Markov Model (FHMM), Artificial Neural Network (ANN), decision tree, etc. In these studies, Deep Neural Networks (DNNs) seem to have certain advantages in both the accuracy and handiness. Ref. [27] proposed a Fully Convolutional Noise Reduction Encoder Algorithm (FCN-dAE) for load disaggregation of non-residential large buildings. This algorithm can train the weight coefficients more effectively in the process of time series modeling. It has a more stable gradient, which simplifies and speeds up the training process. Three difference neural network architectures have been investigated and compared by Kelly and Knottenbelt in [10].

This paper proposes a non-intrusive load disaggregation method that only relies on a single active power measurement at a conventional data acquisition rate. This method requires less measurement and does not require additional installation of hardware and equipment or modification of existing electric energy meters. In terms of the algorithm, this paper is based on the improved Denoising Auto-Encoder algorithm, which can better distinguish loads with similar steady-state power waveforms. Compared with the literature [28], this paper obtains the adjacent maximum value through the maximum pooling operation in the encoding stage, so that the activation function in the analysis window is more independent, and the length of the feature map and the elements of the fully connected layer can also be reduced. Two datasets, i.e., the Reference Energy Disaggregation Dataset (REDD) and TraceBase, are used for test and validation. By numerical test of the real residential data, it proves that the proposed method is superior to the traditional Factorial Hidden Markov Model (FHMM)-based approach. Besides, the proposed method can be used for energy data disaggregation, disregarding the brand and model of each appliance.

This study is organized as follows: Section 2 briefly reviews the four mainstream datasets for NILM, i.e., the REDD, TraceBase, UK-DALE, and Dataport. In Section 3, the proposed disaggregation algorithm is introduced. It elaborates the improvements of the dAE and the two-step procedure of implementing the modified algorithm. Section 4 discusses the test, results, and performance of the proposed method. The proposed DAE network is trained on REDD and TraceBase datasets, and the test results are compared with an FHMM-based approach. Section 5 presents the research conclusions.

2. Dataset Review and Comparison

There are many open-source datasets for non-invasive load disaggregation research worldwide. The commonly used ones are as follows:

(1) **REDD dataset [29]**. Its full name is the Reference Energy Disaggregation Dataset, developed by J. Kolter and M. Johnson of MIT, and is the first dataset for NILM research. The REDD dataset provides high-frequency data sampled at 15 kHz and low-frequency data sampled at 0.5 Hz and 1 Hz. A total of 10 households, 119 days, 268 devices, 1 T electricity consumption data were recorded. Figure 1 is an example of the REDD dataset, showing the electricity usage of various devices in a household over the course of a day. The REDD dataset can be processed with Excel, which is easy to operate. The data download website is: http://redd.csail.mit.edu (accessed on 25 November 2021).

(2) **TraceBase dataset [14]**. The TraceBase dataset was developed by A. Reinhardt of Darmstadt University in Germany. It monitors and records more than ten homes and offices, 31 different types of equipment, 122 devices, and 1270 pieces of load electricity data. Figure 2 shows the electricity consumption of a dishwasher over a period. The entry on the left is time, and the two numbers on the far right represent the average active power consumption within 1 s and 8 s, respectively. The TraceBase dataset is also stored in the form of an Excel table. The format of the data entry is shown in Figure 2. The data download website is: http://www.TraceBase.org (accessed on 25 November 2021).

(3) **UK-DALE dataset [30]**. Developed by J. Kelly and W. Knottenbelt of Imperial College London, the UK-DALE dataset provides 16 kHz energy consumption data for the whole house and 1/6 Hz energy consumption data for a single device. It is the first dataset for load disaggregation in the UK. This dataset recorded the electricity consumption data of five households, one of which was monitored for up to 655 days. The monitoring equipment recorded the active power of a single device as well as the apparent power of the entire house every 6 s, with the voltage and current of three households sampled at 44.1 kHz but reduced to 16 kHz when stored. In addition, the active power, apparent power, and voltage RMS were calculated according to the measured voltage and current, and the calculation frequency was 1 Hz. This dataset is a file in HDF5 (Hierarchical Data Format) format, which needs to be read and analyzed with NILMTK, a non-intrusive load monitoring tool. However, the NILMTK package needs to be loaded and configured with Anaconda software, which is relatively complicated to use.

(4) **Dataport dataset [31]**. The Dataport dataset was developed by Pecan Street company and is the most comprehensive dataset for NILM research. In total, it contains up to 722 households' power consumption data and individual device's power consumption data. Its data sampling rate is low, sampling once a minute. The Dataport dataset is free for member universities, but a paid download is required for commercial use. Like the UK-DALE dataset, this dataset also requires the use of the NILMTK tool for data analysis and statistics.

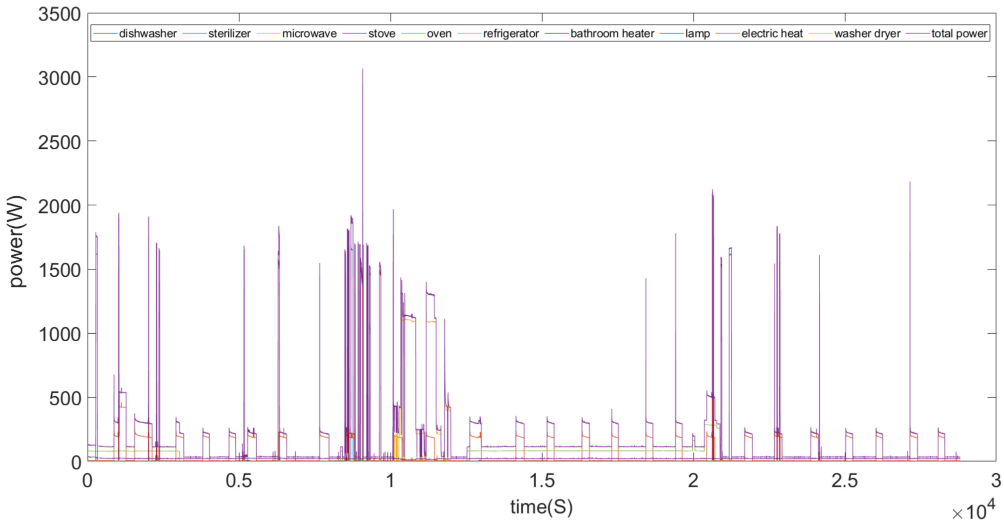

Figure 1. The power waveform of each load in a household in one day.

```
07/02/2012 10:02:35;9;9
07/02/2012 10:02:36;109;23
07/02/2012 10:02:38;104;34
07/02/2012 10:02:39;100;55
07/02/2012 10:02:41;100;79
07/02/2012 10:02:42;98;90
07/02/2012 10:02:44;102;98
07/02/2012 10:02:45;102;98
07/02/2012 10:02:47;107;100
07/02/2012 10:02:48;104;102
```

Figure 2. The data format of the TraceBase dataset.

This paper only uses low-frequency active power data. Considering that the REDD dataset and the TraceBase dataset are relatively simple to use, and the data volume is sufficient for machine learning training, the REDD dataset and the TraceBase dataset are used for sample training and method verification.

3. The Proposed Load Disaggregation Algorithm

Usually, a household has multiple electrical devices turned on at the same time, so its total active power is composed of the sub-power of each electrical device. What we need to do is to extract the power characteristics of each electrical device and use it to separate the individual power consumption from the total power mixture. This separation process can be regarded as noise reduction in image processing or speech recognition. Typical noise reduction treatments include removing noise from old photos, or removing noise from a piece of sound, or even filling in the unclear parts of an image. The essence of load disaggregation is load decomposition. The total mixed power can be regarded as the picture or recording that needs to be processed, and the power generated by other unconcerned equipment can be regarded as "noise".

3.1. Improved Denoising Auto-Encoder Algorithm

The Auto-Encoder algorithm (AE) belongs to unsupervised learning and does not require labeling of training samples. AE consists of a three-layer network. First, the input layer is encoded and compressed, stored in the intermediate layer (or called the encoding layer), and then the intermediate layer is decoded, and a reconstructed new vector is output in the output layer. So, in essence, AE consists of two processes: encoding and decoding. In the encoding process, the deterministic mapping f_θ maps the input vector **x** to a hidden agent **y**, and f_θ is the encoder. A typical encoder adopts the nonlinear affine mapping model shown in Equation (1).

$$f_\theta(\mathbf{x}) = s(\mathbf{Wx} + \mathbf{b}) \quad (1)$$

where θ = {**W**, **b**} represents the parameter set, **W** is the weight matrix of $d' \times d$, and **b** is the offset vector of d′. In the decoding process, the previously obtained hidden agent **y** is mapped back to reconstruct a d-dimensional vector **z** in the input space, $\mathbf{z} = g_{\theta'}(\mathbf{y})$. $g_{\theta'}$ is the decoder. A typical decoder adopts the squeezed nonlinear radial mapping model shown in Equation (2).

$$f_\theta(\mathbf{x}) = s(\mathbf{Wx} + \mathbf{b}) \quad (2)$$

where θ' = {**W′**, **b′**}. The meanings of **W′** and **b′** are similar to those of **W** and **b** in Formula (1). It should be noted that the d-dimensional vector **z** obtained after decoding is not a reconstruction of the input vector **x** in the full sense, but a reconstruction of probability theory, because the probability distribution parameters of p(X | Z = z) (especially its mean) may increase the probability of **x**. One of the simplest compression methods is to reduce the dimensionality of the input vector, so linear AE with only a single hidden layer can be regarded as a special principal component analysis method (PCA). But unlike PCA, AE can contain multiple layers and the network function can be nonlinear.

Denoising Auto-encoder (dAE) is a special autoencoder whose purpose is to separate a "clean" target signal from a noisy input, proposed by P. Vencent et al. in 2008 [32]. The dAE algorithm first artificially adds a random "noise" signal $\widetilde{x}(\widetilde{x} \sim q_D(\tilde{\mathbf{x}}|\mathbf{x}))$ to the input vector **x**. Similar to an auto-encoder, dAE maps the noisy input signal $\widetilde{x}$ to a hidden agent $y = f_\theta(\widetilde{x}) = s(W\widetilde{x} + b)$, which constructs a decoded output vector $\mathbf{z} = g_{\theta'}(\mathbf{y})$. The structure of the denoising autoencoder is shown in Figure 3. The parameters θ and $\theta^{'}$ are trained to minimize the average reconstruction error during training, i.e., to make the output **z** as close as possible to the original uncontaminated input vector **x**, so that **z** is now a deterministic function of $\tilde{\mathbf{x}}$. It is worth noting that although dAE is still to minimize the reconstruction loss between the original input **x** and the reconstructed agent **y**, it still needs to maximize the lower bound of mutual information between the original input **x** and the reconstructed agent **y**. However, at this time **y** is obtained by using deterministic mapping for "polluted" input, so its feature extraction and learning ability is stronger than traditional autoencoders.

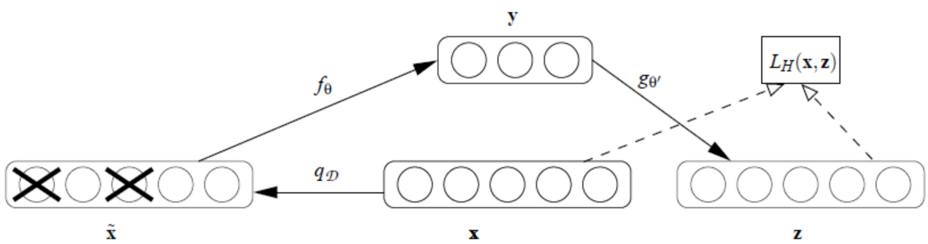

Figure 3. The structure of Denoising Autoencoder (the signal obtained by adding random noise to the original input **x**, f_θ is the encoder, **y** is the intermediate proxy after encoding and mapping, $g_{\theta'}$ is the decoder, **z** is the reconstruction input, and L_H(**x**, **z**) is the reconstruction loss, which is used to measure the reconstruction error).

In the load separation stage, the load identification method based on dAE generally uses a sliding window to analyze the input mixed power signal $y(t)$, and the length of the sliding window is determined by the use time of the corresponding electrical equipment. Therefore, for a mixed power obtained by turning on multiple devices at the same time, the sliding windows will be overlapped. Traditional denoising autoencoder-based load decomposition methods use the average value of the overlapping parts to reconstruct this overlapping window [10]. A problem with this approach is that when a device's on-time is only included in this overlapping window for a small fraction of time, the load identification results can be significantly higher than the actual power usage. As the window slides, the identified error will further increase. Here we use the median filter to process the overlapping part, that is, the output signal of the overlapping part is the result of *y(t)* after median filtering. Specifically, because the power change of the overlapping window is relatively small, the output value of the overlapping window can be replaced by the statistical median of all values in a neighborhood of a certain size. This neighborhood is called a window. The wider the window, the smoother the output will be, but it may also wipe out useful signal features. Therefore, the size of the window should be determined according to the actual hybrid power characteristics.

3.2. Decomposition Steps Based on Improved DAE

The problem of non-intrusive load identification can be expressed by Equation (3).

$$y(t) = \sum_{i=1}^{N} y_i(t) + e(t) \tag{3}$$

where $y_i(t)$ represents the electrical quantity of a single electrical device, and this electrical quantity may be power, voltage, or current. Without loss of generality, we consider it the active power value. $y(t)$ indicates the total electricity consumption of this household. $e(t)$ represents the total measurement error, where we consider the measurement error to be 0. N represents the number of electrical appliances in this household. Therefore, according to Formula (3), the NILM problem is to use the algorithm to obtain the power consumption value of a single electrical device when only the total load power is known. We transform the load decomposition into a noise reduction problem, as shown in Equation (4).

$$y(t) = y_k(t) + c_k(t), \quad k = 1, 2, \ldots, N \tag{4}$$

$$c_k(t) = \sum_{i=1, i\neq k}^{N} y_i(t) \tag{5}$$

where $c_k(t)$ represents the sum of the power of all other devices except device k, and $y_k(t)$ represents the load k that needs to be separated. Therefore, to obtain the value of the active power consumed by the load k of interest, one only needs to separate $c_k(t)$ from the total load $y_k(t)$.

The separation steps based on the improved dAE algorithm are as follows:

Stage 1: Encoding the network:

1. One or more one-dimensional convolutional layers process the original total input power value to generate a set of feature maps;
2. Each convolutional layer sequentially goes through a linear activation function, a maximum pooling layer, an additional convolutional layer, and a pooling layer, and finally forms a fully connected multilayer perceptron;
3. The fully connected layer is processed by the modified linear unit (ReLU) activation function to end the entire encoding process.

Stage 2: Decoding the network:

4. Upsampling the fully connected multilayer perceptron through deconvolution;
5. Up-pooling the results in 4 (the inverse process of max-pooling);
6. Continue to upsample the results in 5 through deconvolution;
7. Obtain the decoded and reconstructed noise reduction signal.

In stage 1 and step 2, the adjacent maxima are obtained through the maximum pooling operation, so that the activation function positions in the analysis window are more independent, and the length of the feature map and the number of fully connected layer elements can also be reduced. The modified linear unit (ReLU) activation function compares the magnitude of the input with zero and outputs a larger value, thereby avoiding negative values of the load power after decomposition. The goal of this modified dAE training network is to minimize the mean squared error (MSE) between the output and the activation function of the device to be separated, using a stochastic gradient descent (SGD) method for training parameter optimization. Unlike traditional dAE, which requires artificially adding noise data to the input data, in NILM research, only the power of non-research objects is used as noise. It can be seen that the noise reduction automatic coding for NILM research is not equivalent to the traditional image or sound noise reduction but uses noise reduction as a training standard to better learn how to extract useful features, so as to better construct high-level acting.

4. Performance Evaluation

In this section, the proposed improved dAE network is trained on the measured data of REDD and TraceBase, and the test results are compared with the factorial Hidden Markov Model (FHMM) algorithm [28]. All codes are in Python language, and NILMTK and Pandas tools are used to analyze the data. The neural network training environment is Win10 Home Edition, Intel i5-10210U processor, 8 G memory, and NVIDIA GeForce MX110 graphics card.

4.1. Performance Metrics

The evaluation of the NILM algorithm can be divided into two aspects: the accuracy of energy decomposition and the correctness of equipment state detection. In terms of energy decomposition, the evaluation indicators are authenticity, accuracy, and F_1 index, which are represented by $R_i^{(E)}$, $P_i^{(E)}$, and $F_1^{(E)}$, respectively. The specific calculation formulas of the first two indicators are shown in Formulas (6) and (7).

$$R_i^{(E)} = \frac{\sum_{t=1}^{T} \min(\hat{y}_i(t), y_i(t))}{\sum_{t=1}^{T} y_i(t)} \tag{6}$$

$$P_i^{(E)} = \frac{\sum_{t=1}^{T} \min(\hat{y}_i(t), y_i(t))}{\sum_{t=1}^{T} \hat{y}_i(t)} \tag{7}$$

where $\hat{y}_i(t)$ represents the separated energy signal, $y_i(t)$ represents the real energy consumption of the device, and T represents the total number of samples. In order to analyze the overall performance of the load disaggregation algorithm, we analyze the average authenticity and accuracy of all equipment, and calculate as follows:

$$R^{(E)} = \frac{1}{N} \sum_{i=1}^{N} R_i^{(E)} \tag{8}$$

$$P^{(E)} = \frac{1}{N} \sum_{i=1}^{N} P_i^{(E)} \tag{9}$$

where $R^{(E)}$ and $P^{(E)}$ represent the average value obtained by considering the authenticity and accuracy of all equipment load resolution, respectively, reflecting the overall performance of the NILM algorithm. The metric $F_1^{(E)}$ is the geometric mean of authenticity and accuracy, calculated as follows:

$$F_1^{(E)} = 2\frac{R^{(E)} P^{(E)}}{R^{(E)} + P^{(E)}} \tag{10}$$

In addition, we also define the standard error NEP of load identification, which is used to represent the sum of the deviation between the equipment energy consumption obtained after decomposition and the standard energy consumption. This deviation sum is normalized by the total real equipment energy consumption, and its calculation formula is:

$$\mathrm{NEP}_i = \frac{\sum_{i=1}^{T} |y_i(t) - \hat{y}_i(t)|}{\sum_{t=1}^{T} y_i(t)} \tag{11}$$

The detection of equipment status refers to the detection of the on/off status of the equipment, which can be decomposed into four indicators, true positive (TP), false positive (FP), false negative (FN), and true negative (TN). The specific definitions of the four indicators are as follows:

$$\mathrm{TP}_i = \sum_{t=1}^{T} (s_i(t) = on, \quad \hat{s}_i(t) = on) \tag{12}$$

$$\mathrm{FP}_i = \sum_{t=1}^{T} (s_i(t) = off, \quad \hat{s}_i(t) = on) \tag{13}$$

$$\mathrm{FN}_i = \sum_{t=1}^{T} (s_i(t) = on, \quad \hat{s}_i(t) = off) \tag{14}$$

$$\mathrm{TN}_i = \sum_{t=1}^{T} (s_i(t) = off, \quad \hat{s}_i(t) = off) \tag{15}$$

In Equations (12)–(15), $s_i(t)$ and $\hat{s}_i(t)$ represent the real state and identification state of the device i at time t, respectively, and on and off represent the two states of the device. The authenticity and accuracy of identification based on device status are defined as:

$$R_i^{(S)} = \frac{\mathrm{TP}_i}{\mathrm{TP}_i + \mathrm{FN}_i}, \quad P_i^{(S)} = \frac{\mathrm{TP}_i}{\mathrm{TP}_i + \mathrm{FP}_i} \tag{16}$$

Similarly, considering the authenticity and accuracy of all equipment status detection and identification, the indicators are obtained:

$$R^{(S)} = \frac{1}{N} \sum_{i=1}^{N} R_i^{(S)}, \quad P^{(S)} = \frac{1}{N} \sum_{i=1}^{N} P_i^{(S)} \tag{17}$$

Thus, the index $F_1^{(S)}$ based on the device state is obtained:

$$F_1^{(S)} = \frac{2R^{(S)} P^{(S)}}{R^{(S)} + P^{(S)}} \tag{18}$$

In addition, we also use the Matthews Correlation Coefficient (MCC) as the identification accuracy index, which is defined as:

$$\mathrm{MCC}_i = \frac{\mathrm{TP}_i \mathrm{TN}_i - \mathrm{FP}_i \mathrm{FN}_i}{\sqrt{(\mathrm{TP}_i + \mathrm{FP}_i)(\mathrm{TP}_i + \mathrm{FN}_i)(\mathrm{TN}_i + \mathrm{FP}_i)(\mathrm{TN}_i + \mathrm{FN}_i)}} \tag{19}$$

The overall Matthews Correlation Coefficient is

$$\mathrm{MCC} = \frac{1}{N} \sum_{i=1}^{N} \mathrm{MCC}_i \tag{20}$$

The value of MCC is in the range of $[-1, 1]$. The larger the value is, the more accurate the identification is, and the value of 0 is a random prediction.

4.2. Test Result

4.2.1. Performance Test Using REDD Dataset

In this REDD dataset, Household 1 and Household 2 data were selected as test subjects. The data is updated every 3 s, so it contains a total of 28,800 pieces of data in one day. In order to verify the effectiveness of the proposed dAE-based algorithm, we tested and compared the load decomposition effects of 10 kinds of electrical equipment in Household 1 and 8 kinds of electrical equipment in Household 2, respectively. Among them, the 10 kinds of electrical equipment in family 1 are oven, refrigerator, dishwasher, sterilizer, lamp, dryer, microwave oven, bathroom heater, electric heater, stove. The 8 kinds of electrical equipment in Household 2 are kitchen appliance 1, kitchen appliances 2, lamp, stove, microwave, dryer, refrigerator, dishwasher.

In the process of data training, considering that the device may show different power waveforms in different time periods, for each device, 10 days of data are selected for training, and the other 10 days of data are used for testing and verification. Therefore, a total of 576,000 pieces of data are used. In the REDD dataset, the power consumption data of all 10 electrical devices exceeds 600,000.

To keep it concise, only the power decomposition results of three electrical appliances in Household 1 are presented, namely dishwasher, refrigerator, and lamp (shown in Figure 4). The abscissa in the figure is the time, and the unit is seconds. Because we hope to better observe the load disaggregation effect of the improved dAE algorithm and the FHMM algorithm, only the power waveform during the time when the device is turned on is selected, so the abscissa time only lasts for 6000 s, that is 2000 data points. In Figure 4, the waveform of line 1 represents the actual power curve of the load, the waveform of line 2 represents the load identification result based on the improved dAE algorithm, the waveform of line 3 represents the load identification result based on the standard DAE algorithm, and the waveform of line 4 represents the load identification result based on the FHMM algorithm.

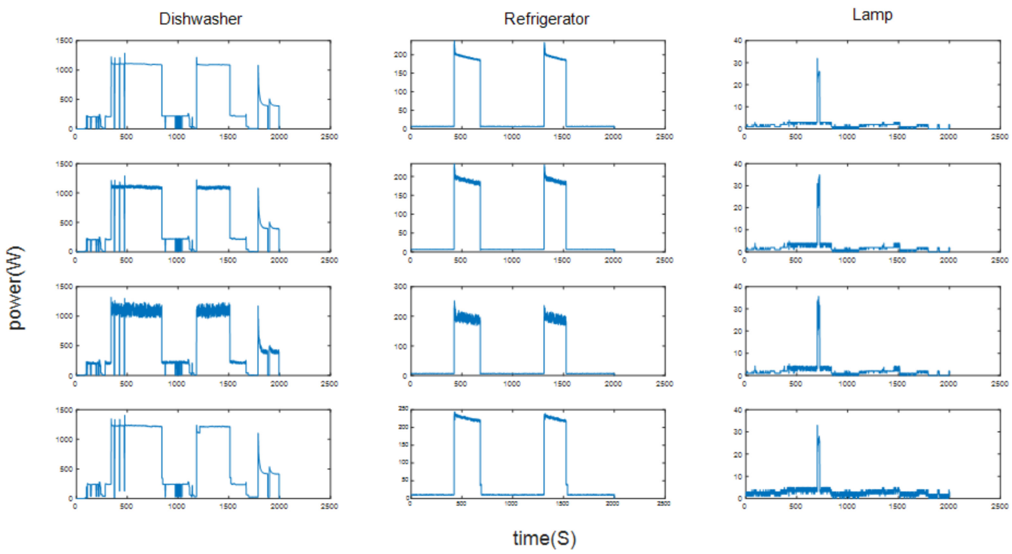

Figure 4. Identification results of three devices in home 1. (Line 1: the actual power curve of the load; Line 2: the load identification result based on the improved dAE algorithm; Line 3: the load identification result based on the standard dAE algorithm; Line 4: the load identification result based on the FHMM algorithm).

It should be noted that commonly used household electrical equipment can be divided into three categories from the operating state: single state class, continuous change class, and multi-state class:

Single state class: This means that there is only one stable state after the device is turned on, and the power generally remains unchanged, such as lamps, kettles, microwave ovens, etc.

Continuous change type: This means that the power of the device will have a continuous increase/decrease process during the process of turning on/off, such as TV (power change 50 W–75 W), computer (80 W–100 W), etc.

Multi-state class: Refers to the device having multiple power states during operation, such as refrigerators, washing machines, dishwashers, dryers, etc.

Among these three types of electrical equipment, the identification of single-state and continuous-change types is relatively simple, while the multi-state type is easily confused with other equipment due to its great difference in power in different state stages.

As can be seen from Figure 4, for lamps belonging to the single-state category, the identification effects of the three algorithms are good, which can well reflect the on and off states of the device, and the calculation of the power consumption value is also relatively accurate. For the dishwashers and refrigerators belonging to the multi-state category, the load identification effect based on the improved dAE algorithm is better, which is reflected in two aspects: (1) It decomposes the real power consumption value of the equipment more accurately; (2) It detects the different state stages of the equipment more accurately, thereby reducing the probability of misjudgment.

Figure 5 shows the usage of the dishwasher in Household 1 on a certain day, and its usage time is in the interval of 10,000–12,000 s. This interval is enlarged and the identification results of the two algorithms are compared, as shown in Figure 6.

It can be clearly seen from the figure that the load identification algorithm based on the improved dAE only has a little jitter in the high-power operation state; the jitter error does not exceed 5%, and can well fit the switching process between the states. Overall, the identification method based on FHMM has a higher power decomposition result; the amplitude is close to 20% and cannot accurately represent the load switching process. The result from standard dAE is also included for comparison, from which we can see that it has much more fluctuation. Especially at the time 1100 s, there is a big spike.

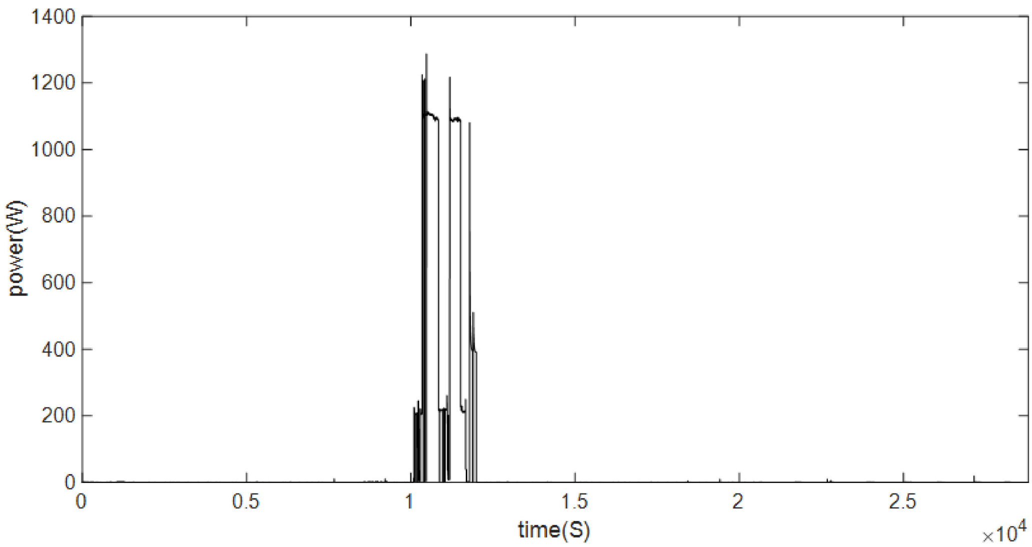

Figure 5. The actual daily energy consumption of Household 1’s dishwasher.

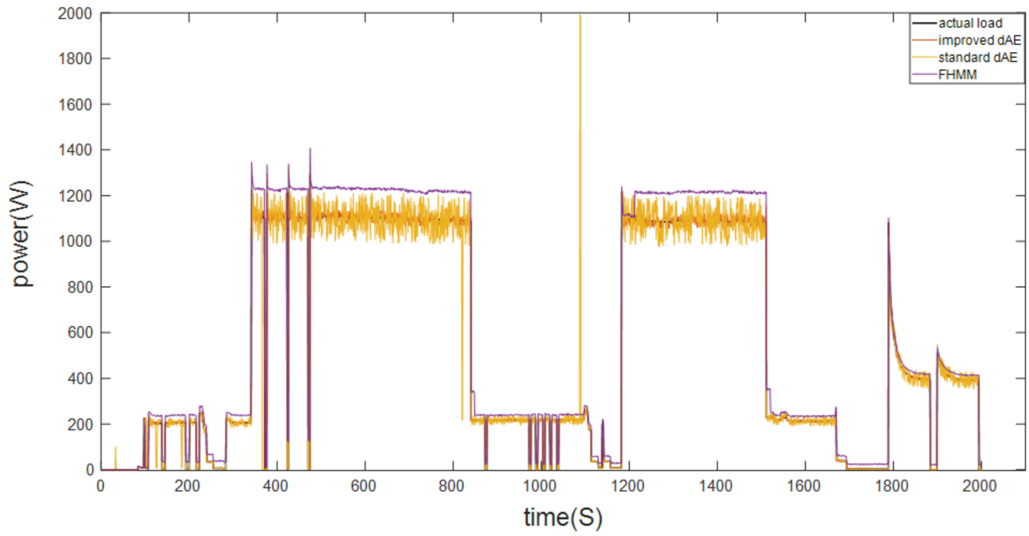

Figure 6. Actual energy consumption of dishwasher in Household 1 in one day.

Table 1 compares the four indicators of the three algorithms. These four indicators are defined and explained in Section 4.1. They represent the accuracy of energy consumption disaggregation (the bigger the better), the accuracy of the device status detection (the bigger the better), the NEP, which represents the deviation of the power disaggregation result from the actual value (the smaller the better), and the Matthews Correlation Coefficient (MCC), which represents the accuracy of the state detection (the closer to 1 the better). Due to space limitations, the table only lists the comparison of 5 kinds of equipment. It can be seen from the table that all indicators obtained by the improved dAE algorithm are better than the FHMM algorithm. The percentage of improvement regarding improved dAE and standard dAE is listed on the far-right side of the table, and the bold font indicates better performance of the proposed algorithm.

Table 1. Comparison of identification indexes of several equipment using REDD dataset.

Algorithm	Index	Oven	Refrigerator	Dish Washer	Lamp	Washer Dryer	Overall Performance	Improvement *
FHMM	$F_1^{(E)}\%$	33.2	22.7	50.0	45.3	80.3	46.30	
	$F_1^{(S)}\%$	78.6	42.6	21.5	36.3	52.3	46.26	
	NEP	2.652	0.709	3.222	1.562	0.441	1.7172	
	MCC	0.223	0.420	0.478	0.423	0.652	0.4392	
Standard dAE	$F_1^{(E)}\%$	42.6	45.6	70.5	59.6	85.4	60.74	
	$F_1^{(S)}\%$	82.6	58.1	44.9	55.0	66.2	61.36	
	NEP	1.852	0.652	1.256	1.006	0.333	1.020	
	MCC	0.455	0.558	0.658	0.455	0.742	0.574	
Improved dAE	$F_1^{(E)}\%$	78.5	66.84	88.8	69.0	99.3	80.50	**32.5%**
	$F_1^{(S)}\%$	92.3	65.96	65.3	67.5	74.5	73.11	**19.1%**
	NEP	0.389	0.520	0.226	0.265	0.225	0.325	**68.1%**
	MCC	0.674	0.685	0.783	0.885	0.898	0.785	**36.8%**

* percentage of improvement regarding the improved dAE and standard dAE.

Due to the variety of types of household electrical appliances, there may be differences in the power consumption behavior of different types of equipment. To test the generality of the algorithm, we trained the network using the data of Household 1, Household 3, and Household 4, and the trained network decomposes the ensemble power of Household 2. Figure 7 shows the results of identifying each device in Household 2 after using the data of Household 1 for network training. Due to space limitations, only the comparison results of three devices are shown, namely stove, microwave, and sterilizer. In Figure 7, the waveform of line 1 represents the actual power curve of the load, the waveform of line 2 represents the load identification result based on the improved dAE algorithm, the waveform of line 3 represents the load identification result based on the standard dAE algorithm, and the waveform of line 4 represents the load identification result based on the FHMM algorithm. It can be seen from the figure that, for single-state microwave ovens and sterilizers, all three algorithms can properly identify the equipment, while for stoves with multiple states, the improved dAE algorithm is obviously better than the standard dAE or FHMM algorithm.

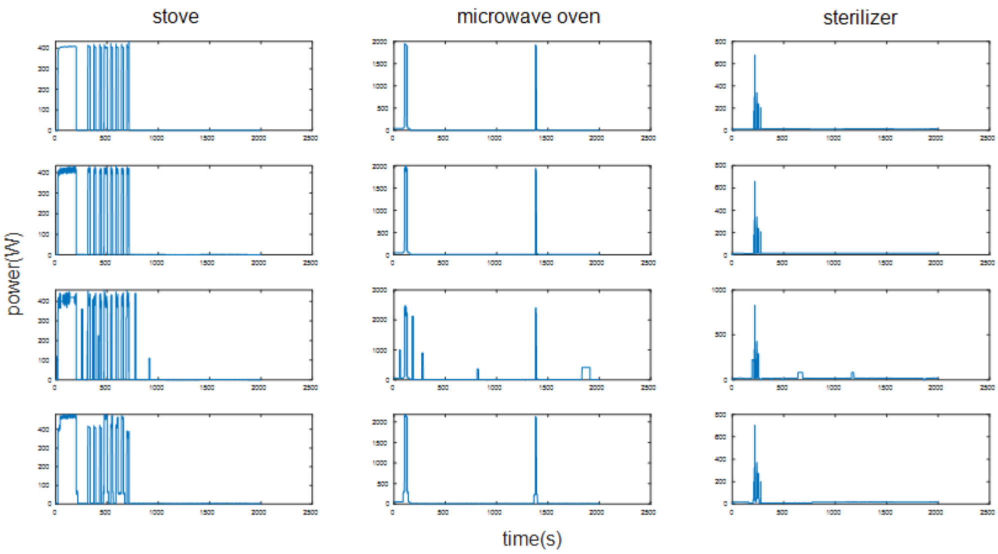

Figure 7. Identification result of Household 2 after using the network trained by dataset of Household 1 (Line 1: the actual power curve of the load; Line 2: the load identification result based on the improved dAE algorithm; Line 3: the load identification result based on the standard dAE algorithm; Line 4: the load identification result based on the FHMM algorithm).

4.2.2. Performance Test Using TraceBase Dataset

The TraceBase dataset contains 31 different types of devices, 122 devices, and 1270 pieces of load power consumption data. The data collection interval is 1–2 s. We used two algorithms to identify 20 of these devices, and selected the identification results of TV sets, desktop computers, and electric irons to display, as shown in Figure 8. In order to better illustrate the pattern of electric iron, the abscissa axis is truncated from time 0 to 800 s because the power assumption is 0 afterwards. As can be seen from the figure, the improved dAE algorithm has obvious advantages in both identifying the power consumption of the real equipment and detecting the different stages of the equipment.

Figure 9 compares the recognition performance of the three algorithms on a desktop computer from 15,000 s to 25,000 s. It can be seen from the figure that the jitter error of the load identification algorithm based on the improved dAE does not exceed 4%, and it can well fit the switching process between states, while the decomposition method based on standard dAE and FHMM are not accurate at the time of load start and stop. Additionally, the overall decomposed load power is too high. Table 2 compares the four indexes of the three algorithms. It can be seen from the table that all indicators obtained by the improved dAE algorithm are better than the standard dAE or FHMM algorithm, and the overall performance value is listed on the second far-right side of the table.

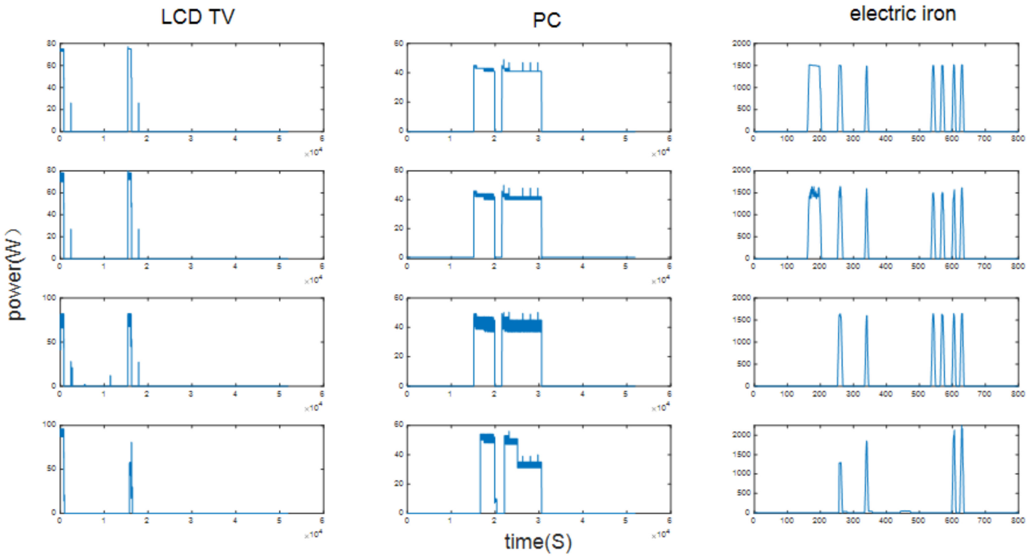

Figure 8. Identification Results of the three devices in TraceBase. (Line 1: the actual power curve of the load; Line 2: the load identification result based on the improved dAE algorithm; Line 3: the load identification result based on the standard dAE algorithm; Line 4: the load identification result based on the FHMM algorithm).

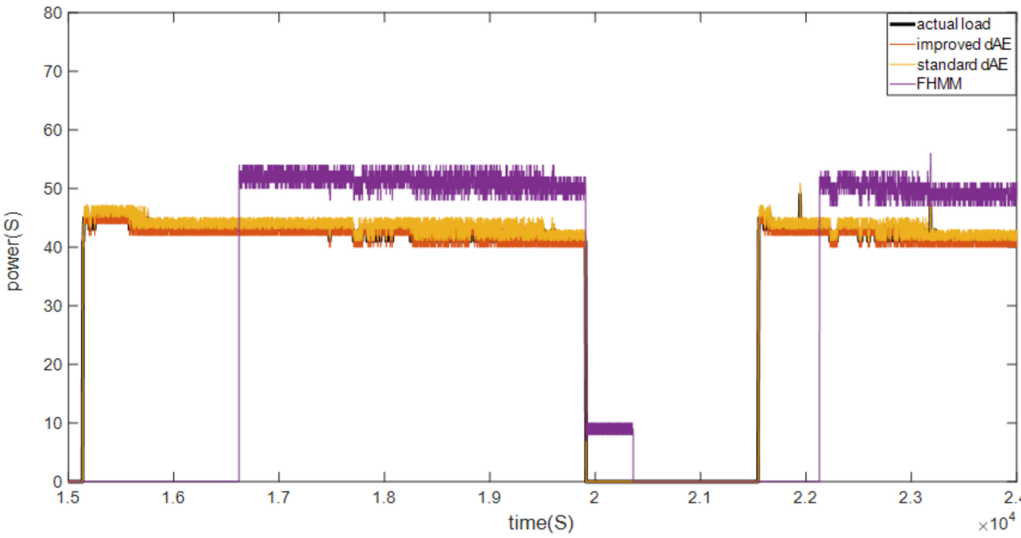

Figure 9. PC load identification results over a period of 15,000–25,000 s.

Table 2. Comparison of identification indexes of several equipment using TraceBase dataset.

Algorithm	Index	Coffee Machine	LCD-TV	Desktop	Wash Machine	Electric Iron	Overall Performance	Improvement *
FHMM	$F_1^{(E)}\%$	65.6	45.3	33.3	35.9	39.6	43.94	
	$F_1^{(S)}\%$	60.4	56.3	35.6	52.52	54.1	51.784	
	NEP	0.744	0.523	2.250	6.235	9.601	3.8706	
	MCC	0.732	0.729	0.420	0.452	0.333	0.5332	
Standard dAE	$F_1^{(E)}\%$	74.2	66.6	44.3	55.2	52.3	58.52	
	$F_1^{(S)}\%$	71.0	74.2	45.3	62.3	65.4	63.64	
	NEP	0.653	0.387	2.023	5.236	6.200	2.9000	
	MCC	0.741	0.774	0.625	0.650	0.661	0.6902	

Table 2. *Cont.*

Algorithm	Index	Coffee Machine	LCD-TV	Desktop	Wash Machine	Electric Iron	Overall Performance	Improvement *
Improved dAE	$F_1^{(E)}\%$	87.3	77.6	55.6	65.2	87.6	**74.66**	**27.60%**
	$F_1^{(S)}\%$	88.9	85.3	65.4	72.3	74.1	**77.20**	**21.30%**
	NEP	0.520	0.125	1.985	1.690	3.652	**1.5944**	**45.00%**
	MCC	0.812	0.874	0.898	0.870	0.704	**0.8316**	**20.50%**

* percentage of improvement regarding the improved dAE and standard dAE.

5. Conclusions

This paper proposes a non-intrusive load identification method that only relies on single active power measurements at a conventional sampling rate. This method is based on the Denoising Auto-Encoder (dAE) algorithm, which regards the total mixing power as a picture or a recording that needs to be processed, and the power generated by other unconcerned devices as "noise". The load power of the individual equipment is disaggregated from the total mixed power.

In the performance evaluation test, the REDD and TraceBase datasets are used to compare the effectiveness between the proposed method and the Factorial Hidden Markov Model (FHMM) algorithm, and four specific metrics for power disaggregation and state detection performance are introduced. The test results show that the proposed method has obvious advantages in both identifying the actual power consumption of the device and detecting the state of the device. In addition, the proposed algorithm has good generality and can effectively identify the same equipment of different models or brands.

Author Contributions: Conceptualization, methodology, X.H.; software, validation, X.H. and H.D.; data curation, manuscript review and revision, W.Y. and J.H. All authors have read and agreed to the published version of the manuscript.

Funding: This research was funded by Provincial Science and Technology Joint Fund Project, 2021–2023, grant number 2021JJ50082.

Institutional Review Board Statement: Not applicable.

Informed Consent Statement: Not applicable.

Data Availability Statement: Not applicable.

Conflicts of Interest: The authors declare no conflict of interest.

References

1. Ruano, A.; Hernandez, A.; Ureña, J.; Ruano, M.; Garcia, J. NILM techniques for intelligent home energy management and ambient assisted living: A review. *Energies* **2019**, *12*, 2203. [CrossRef]
2. Sadeghianpourhamami, N.; Ruyssinck, J.; Deschrijver, D.; Dhaene, T.; Develder, C. Comprehensive feature selection for appliance classification in NILM. *Energy Build.* **2017**, *151*, 98–106. [CrossRef]
3. Figueiredo, M.B.; Almeida, A.; Ribeiro, B. An Experimental Study on Electrical Signature Identification of Non-Intrusive Load Monitoring (Nilm) Systems. In Proceedings of the International Conference on Adaptive and Natural Computing Algorithms, Ljubljana, Slovenia, 14–16 April 2011; Springer: Berlin/Heidelberg, Germany, 2011; pp. 31–40.
4. Bouhouras, A.S.; Gkaidatzis, P.A.; Panagiotou, E.; Poulakis, N.; Christoforidis, G. CA NILM algorithm with enhanced disaggregation scheme under harmonic current vectors. *Energy Build.* **2019**, *183*, 392–407. [CrossRef]
5. Tu, C.; He, X.; Shuai, Z.; Jiang, F. Big data issues in smart grid—A review. *Renew. Sustain. Energy Rev.* **2017**, *79*, 1099–1107. [CrossRef]
6. Biansoongnern, S.; Plangklang, B. Nonintrusive load monitoring (NILM) using an Artificial Neural Network in embedded system with low sampling rate. In Proceedings of the 2016 13th International Conference on Electrical Engineering/Electronics, Computer, Telecommunications and Information Technology (ECTI-CON), Chiang Mai, Thailand, 28 June–1 July 2016; IEEE: Piscataway, NJ, USA, 2016; pp. 1–4.
7. Huber, P.; Calatroni, A.; Rumsch, A.; Paice, A. Review on deep neural networks applied to low-frequency nilm. *Energies* **2021**, *14*, 2390. [CrossRef]

8. Revuelta Herrero, J.; Lozano Murciego, Á.; López Barriuso, A.; Hernández de la Iglesia, D.; Villarrubia González, G.; Corchado Rodríguez, J.M.; Carreira, R. Non Intrusive Load Monitoring (Nilm): A State of the Art. In Proceedings of the International Conference on Practical Applications of Agents and Multi-Agent Systems, Porto, Portugal, 21–23 June 2017; Springer: Cham, Switzerland, 2017; pp. 125–138.
9. Machlev, R.; Tolkachov, D.; Levron, Y.; Beck, Y. Dimension reduction for NILM classification based on principle component analysis. *Electr. Power Syst. Res.* **2020**, *187*, 106459. [CrossRef]
10. Kelly, J.; Knottenbelt, W. Neural nilm: Deep neural networks applied to energy disaggregation. In Proceedings of the 2nd ACM International Conference on Embedded Systems for Energy-Efficient Built Environments, Seoul, Korea, 4–5 November 2015; pp. 55–64.
11. Batra, N.; Singh, A.; Whitehouse, K. Neighbourhood nilm: A big-data approach to household energy disaggregation. *arXiv* **2015**, arXiv:1511.02900.
12. Nalmpantis, C.; Vrakas, D. Machine learning approaches for non-intrusive load monitoring: From qualitative to quantitative comparation. *Artif. Intell. Rev.* **2019**, *52*, 217–243. [CrossRef]
13. Yang, F.; Liu, B.; Luan, W.; Zhao, B.; Liu, Z.; Xiao, X.; Zhang, R. FHMM Based Industrial Load Disaggregation. In Proceedings of the 2021 6th Asia Conference on Power and Electrical Engineering (ACPEE), Chongqing, China, 8–11 April 2021; IEEE: Piscataway, NJ, USA, 2021; pp. 330–334.
14. Reinhardt, A.; Baumann, P.; Burgstahler, D.; Hollick, M.; Chonov, H.; Werner, M.; Steinmetz, R. On the accuracy of appliance identification based on distributed load metering data. In Proceedings of the IFIP Conference on Sustainable Internet & Ict for Sustainability, Pisa, Italy, 4–5 October 2012; IEEE Computer Society: Washington, DC, USA, 2012.
15. Bouhouras, A.S.; Milioudis, A.N.; Labridis, D.P. Development of distinct load signatures for higher efficiency of NILM algorithms. *Electr. Power Syst. Res.* **2014**, *117*, 163–171. [CrossRef]
16. Desai, S.; Alhadad, R.; Mahmood, A.; Chilamkurti, N.; Rho, S. Multi-state energy classifier to evaluate the performance of the nilm algorithm. *Sensors* **2019**, *19*, 5236. [CrossRef]
17. Puente, C.; Palacios, R.; González-Arechavala, Y.; Sánchez-Úbeda, E.F. Non-intrusive load monitoring (NILM) for energy disaggregation using soft computing techniques. *Energies* **2020**, *13*, 3117. [CrossRef]
18. Dinesh, C.; Nettasinghe, B.W.; Godaliyadda, R.I.; Ekanayake MP, B.; Ekanayake, J.; Wijayakulasooriya, J.V. Residential appliance identification based on spectral information of low frequency smart meter measurements. *IEEE Trans. Smart Grid* **2016**, *7*, 2781–2792. [CrossRef]
19. Gillis, J.M.; Morsi, W.G. Non-intrusive load monitoring using semi-supervised machine learning and wavelet design. *IEEE Trans. Smart Grid* **2017**, *8*, 2648–2655. [CrossRef]
20. Li, D.; Dick, S. Non-intrusive load monitoring using multi-label classification methods. *Electr. Eng.* **2020**, *103*, 607–619. [CrossRef]
21. Ahmadi, H.; Marti, J.R. Load decomposition at smart meters level using eigenloads approach. *IEEE Trans. Power. Syst.* **2015**, *30*, 3425–3436. [CrossRef]
22. Cominola, A.; Giuliani, M.; Piga, D.; Castelletti, A.; Rizzoli, A.E. A hybrid signature-based iterative disaggregation algorithm for non-intrusive load monitoring. *Appl. Energy.* **2017**, *185*, 331–344. [CrossRef]
23. Makonin, S.; Popowich, F.; Bajić, I.V.; Gill, B.; Bartram, L. Exploiting hmm sparsity to perform online real-time nonintrusive load monitoring. *IEEE Trans. Smart Grid* **2016**, *7*, 2575–2585. [CrossRef]
24. Tsai, M.S.; Lin, Y.H. Modern development of an adaptive non-intrusive appliance load monitoring system in electricity energy conservation. *Appl. Energy* **2012**, *96*, 55–73. [CrossRef]
25. Mauch, L.; Yang, B. A new approach for supervised power disaggregation by using a deep recurrent LSTM network. In Proceedings of the 2015 IEEE Global Conference on Signal and Information Processing (GlobalSIP), Orlando, FL, USA, 14–16 December 2015; pp. 63–67.
26. Figueiredo, M.; De Almeida, A.; Ribeiro, B. Home electrical signal disaggregation for non-intrusive load monitoring (NILM) systems. *Neurocomputing* **2012**, *96*, 66–73. [CrossRef]
27. García-Pérez, D.; Pérez-López, D.; Díaz-Blanco, I.; González-Muñiz, A.; Domínguez-González, M.; Vega AA, C. Fully-convolutional denoising auto-encoders for NILM in large non-residential buildings. *IEEE Trans. Smart Grid* **2020**, *12*, 2722–2731. [CrossRef]
28. Bonfigli, R.; Felicetti, A.; Principi, E.; Fagiani, M.; Squartini, S.; Piazza, F. Denoising autoencoders for non-intrusive load monitoring: Improvements and comparative evaluation. *Energy Build.* **2018**, *158*, 1461–1474. [CrossRef]
29. Kolter, J.Z.; Johnson, M.J. REDD: A public data set for energy disaggregation research. *Artif. Intell.* **2011**, *25*, 59–62.
30. Kelly, J.; Knottenbelt, W. The UK-DALE dataset, domestic appliance-level electricity demand and whole-house demand from five UK homes. *Sci. Data* **2015**, *2*, 150007. [CrossRef] [PubMed]
31. Parson, O.; Fisher, G.; Hersey, A.; Batra, N. Dataport and NILMTK: A building data set designed for non-intrusive load monitoring. In Proceedings of the 3rd IEEE Global Conference on Signal & Information Processing, Orlando, FL, USA, 14–16 December 2015; IEEE: Piscataway, NJ, USA, 2015; pp. 210–214.
32. Vincent, P.; Larochelle, H.; Lajoie, I.; Bengio, Y.; Manzagol, P.A.; Bottou, L. Stacked denoising autoencoders: Learning useful representations in a deep network with a local denoising criterion. *J. Mach. Learn. Res.* **2010**, *11*, 3371–3408.